

Outflows of stars due to quasar feedback

Kastytis Zubovas¹, Sergei Nayakshin¹, Sergey Sazonov^{2,3} and Rashid Sunyaev^{3,2}

¹ *Department of Physics & Astronomy, University of Leicester, Leicester, LE1 7RH, UK*

² *Space Research Institute, Russian Academy of Sciences, Profsoyuznaya 84/32, Moscow 117997, Russia*

³ *Max-Planck-Institut für Astrophysik, Karl-Schwarzschild-Str. 1, Garching 85741, Germany*

E-mail: Kastytis.Zubovas@le.ac.uk

Received

ABSTRACT

Quasar feedback outflows are commonly invoked to drive gas out of galaxies in the early gas-rich epoch to terminate growth of galaxies. Here we present simulations that show that AGN feedback may drive not only gas but also stars out of their host galaxies under certain conditions. The mechanics of this process is as following: (1) AGN-driven outflows accelerate and compress gas filling the host galaxy; (2) the accelerated dense shells become gravitationally unstable and form stars on radial trajectories. For the spherically symmetric initial conditions explored here, the black hole needs to exceed the host's M_σ mass by a factor of a few to accelerate the shells and the new stars to escape velocities. We discuss potential implications of these effects for the host galaxies: (i) radial mixing of bulge stars with the rest of the host; (ii) contribution of quasar outflows to galactic fountains as sources of high-velocity clouds; (iii) wholesale ejection of hyper velocity stars out of their hosts, giving rise to type II supernovae on galactic outskirts, and contributing to reionisation and metal enrichment of the Universe; (iv) bulge erosion and even complete destruction in extreme cases resulting in overweight or bulgeless SMBHs.

Key words: galaxies: evolution - quasars: general - accretion, accretion discs - stars: hypervelocity stars

1 INTRODUCTION

Super-massive black holes (SMBH) accreting gas at rates comparable to the Eddington accretion rate are believed to power quasars. They are expected to launch powerful winds (Shakura & Sunyaev 1973; King 2003; Proga 2003). Such winds are consistent with the fast $v_{\text{out}} \sim 0.1c$ winds detected via absorption (e.g., Pounds et al. 2003a,b) and also recently in emission (Pounds & Vaughan 2011) in AGN X-ray spectra. These nuclear (most likely $R \lesssim 1$ pc) winds must be wide-angle to explain their detection frequency (Tombsi et al. 2010a,b), and energetically should be capable of driving outflows clearing significant fractions of *all* gas of the parent galaxy out (Silk & Rees 1998; King 2005; Zubovas & King 2012a). Recent observations detect such kpc-scale neutral and ionized outflows with outflow velocities of ~ 1000 km s⁻¹ and mass outflow rates of hundreds to thousands of M_\odot yr⁻¹ (e.g., Feruglio et al. 2010; Sturm et al. 2011; Rupke & Veilleux 2011), which are best interpreted as the mass-loaded nuclear outflows. These outflows have wide-ranging implications for galaxy formation and evolution (Di Matteo et al. 2005).

Recently, Nayakshin & Zubovas (2012, hereafter NZ12) have shown that quasar outflows affect the ambient gas in the bulge of the host galaxy in two different ways depending

on whether the ambient shocked gas is able to cool rapidly or not. In the gas-poor epoch, e.g., the present day bulge of the Milky Way, the shocked gas cools slowly, so the shock is approximately adiabatic. The layer of the shocked gas is then geometrically thick and the density in it is ~ 4 times higher than the pre-shock density, as in the strong-shock limit. In contrast, in the gas-rich epoch, when the pre-shock gas density in the bulge is higher, the shocked gas cools more rapidly than the shock can propagate through the bulge. The shocked gas is then swept up into a geometrically thin shell, and the density in the shell is roughly v_e^2/c_s^2 times the pre-shock density, where $v_e \sim 1000$ km s⁻¹ and $c_s \lesssim 10$ km s⁻¹ are the shock front velocity and the sound speed in the shell, respectively. If the pre-shock gas density is a $\gtrsim 0.1$ fraction of the total density responsible for the potential, the swept up shell density is orders of magnitude higher than the tidal density. Unsurprisingly then, NZ12 found that the shell can fragment into star-forming clumps.

Such positive AGN feedback has been explored before with regard to jet interaction with clumpy interstellar medium (Gaibler et al. 2012; Silk et al. 2012). These authors found that AGN jets can also enhance star formation in their host galaxies. However, the details of that process are markedly different from what consider here and so we do

not attempt to draw direct comparison with these previous studies.

NZ12 concentrated on conditions when the shell stalls and falls back on to the SMBH, which physically corresponds to black hole masses below the M_σ mass (King 2003, 2005)

$$M_\sigma \simeq 3.67 \times 10^8 f \sigma_{200}^4 M_\odot, \quad (1)$$

where σ_{200} is the velocity dispersion in the host galaxy bulge, in units of 200 km/s, and f is the ratio of the gas density in the bulge to the total density in the bulge, scaled to the cosmological ratio of 0.16. Here we probe the evolution of the outflow for $M_{\text{bh}} \gtrsim M_\sigma$. We find that the instability leading to the shell fragmentation is still effective when the shell is being driven outward at velocities as large as $\gtrsim 1000$ km s⁻¹, leading to formation of self-gravitating dense gas clumps, and eventually newly born stars, moving radially outward with these high velocities. This result suggests that quasar outflows could not only be expelling gas from the host galaxies but also making some stars by strong compression of that material; since the material is streaming away at high velocity the new stars are born with that velocity as well.

Below we present numerical simulations that exemplify these effects and also consider their theoretical implications.

2 NUMERICAL METHODS

The simulations presented here to demonstrate our main point are set up in the manner identical to those presented in NZ12, so we only briefly overview the setup. For simplicity, the host galaxy is modelled by a fixed singular isothermal sphere potential softened in the central 10 pc where the SMBH is located. The ambient gas is initialised as a sphere with inner radius $R_{\text{in}} = 200$ pc and outer radius $R_{\text{out}} = 10R_{\text{in}}$, at rest, and with the density profile given by $\rho_g(R) = f_g \rho_0(R) = f_g \sigma^2 / 2\pi GR^2$; $\sigma = 141$ km s⁻¹ is the velocity dispersion of the potential and $f_g = 0.16f$ is the ratio of the gas density to the underlying density of stars and dark matter; we choose $f = 1$ for the simulations presented in this paper. We use 5×10^5 SPH particles in each simulation, giving a mass resolution $M_{\text{res}} \simeq 40m_{\text{SPH}} = 2 \times 10^5 M_\odot$, much better than in a typical galaxy-wide AGN feedback simulations (e.g. $M_{\text{res}} \simeq 6 \times 10^6 M_\odot$ in Springel et al. 2005, and much larger than this in cosmological simulations). Initial gas temperature is set such that the sound speed is equal to σ . At time $t = 0$, the quasar outflow is turned on. The critical M_σ mass above which even a purely momentum-driven SMBH outflow should expel the gas for this potential is $M_\sigma \approx 1.5 \times 10^8 f M_\odot$ (Nayakshin & Power 2010). Quasar feedback is implemented via “virtual particles” emitted isotropically by the SMBH (Nayakshin et al. 2009; Nayakshin & Power 2010; Zubovas & Nayakshin 2012). The quasar momentum outflow rate is fixed at L_{Edd}/c and the energy input into the gas is $= 0.05L_{\text{Edd}}$; we use a smooth transition between the momentum- and energy-driven flow regimes, with the cooling radius (Zubovas & King 2012b) $R_c = 500$ pc. The SMBH mass is fixed for the duration of a simulation; this is a reasonable assumption, given that the timescales we are interested in are shorter than the Salpeter time (≈ 40 Myrs). Physically this situation could be realised by a small scale dense gas disc feeding the SMBH at close to its Eddington rate (small scale gas discs are much more

resilient to quasar feedback than extended spherical distributions; see Nayakshin et al. 2012).

Since we are modelling the inner parts of a single galaxy, we can afford a higher numerical resolution, as already noted above. Therefore, we treat star formation in a way similar¹ to that introduced in Nayakshin et al. (2007). Our approach is different from the industry practice (e.g., Springel et al. 2005; Booth & Schaye 2009; Dubois et al. 2012) in modelling star formation in cosmological simulation, where (i) a threshold density for star formation is introduced (ranging from 10^4 to 1 Hydrogen atom per cm³, typically); and (ii) once gas density exceeds the threshold stars are introduced *stochastically* following the 3D form of the Schmidt-Kennicutt law (Kennicutt 1998). This method for treating star formation is reasonable on galaxy-wide scales, provided that the threshold density exceeds the mean gas density by a large factor. However, the method will fail in the inner parts of bulges where the tidal density, $\rho_t = \sigma^2 / (2\pi GR^2) \simeq 10^{-22} R_{\text{kpc}}^{-2} \text{ g cm}^{-3} \simeq 100 R_{\text{kpc}}^{-2} \text{ cm}^{-3}$ is a strong function of radius R and may be higher than the threshold density. We also note that in the standard prescription, once the *mean* gas density exceeds the density threshold then stars are introduced everywhere in this prescription, even in gas regions that are not gravitationally self-bound, e.g., in the hot interclump medium.

Our method avoids these potential pitfalls. Firstly, we require that the gas is self-bound before star formation is initiated. This is done by requiring that the Jeans mass, $M_J \simeq 2.6 \times 10^6 T_4^{3/2} n_4^{-1/2} M_\odot$, exceeds the minimum resolvable mass of the simulation, i.e., that of 40 SPH particles, $m_{\text{res}} = 2 \times 10^5 M_\odot$; here $T_4 = T / (10^4 \text{ K})$ and $n_4 = n / (10^4 \text{ cm}^{-3})$. This criterion stops spurious star formation in dense but hot gas (if such is formed in a strong shock, for example). Secondly, we require that the gas density should exceed the tidal density by a large factor, $A = 200$. The latter is a free parameter, but we tested that the results change insignificantly as long as A is large, by running a set of identical tests in which A was varied from 2 to 200. Physically, this second condition prevents star formation in regions that appear to be self-gravitating but are not dense enough to withstand galactic or bulge tides.

We are therefore confident that our methods correctly capture the onset of star formation, and do this better than the industry standard. However, due to our focus on the effects of AGN feedback, we neglect star formation feedback within the gas clumps. The result of this approximation is that once star formation occurs within the clump it is likely to consume all the available gas, resulting in up to 100% efficiency of star formation. This is most likely incorrect. Star formation feedback could disrupt the star forming clumps or heat them up, limiting star formation efficiency (although we note that the star forming phase of our simulations is quite short, from a few Myr to ~ 10 Myr, so only the most massive stars would have been able to produce supernovae quickly enough). Concluding this discussion, our methods

¹ Although due to a much poorer mass resolution here we do not attempt to model detail of sub-Solar protostar evolution, such as potential mergers of “First Cores” (Larson 1969) or gas accretion onto the sink particles. Such microphysics of star formation is beyond the numerical realm of this paper.

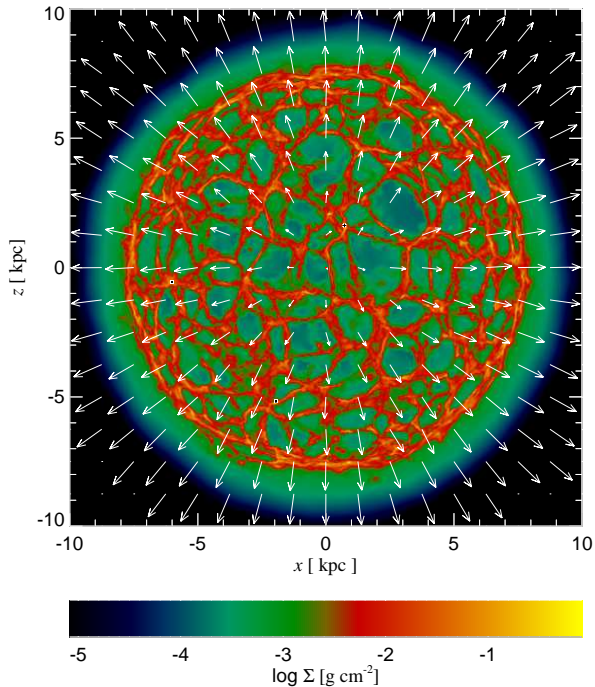


Figure 1. The gas column density and velocity map for simulation M5, 11.8 Myr after the beginning of the simulation. Colour represents projected gas column density (scale at the bottom) and arrows indicate gas velocity. The arrows are logarithmically scaled to the longest one, so they only give qualitative information about gas motions.

correctly predict when star formation occurs, but we probably strongly over-estimate the amount of stars formed. We shall keep this conclusion in mind and come back to it in section 3.

Here we present three simulations, M1, M2 and M5, where the number indicates the mass of the SMBH in units of $10^8 M_{\odot}$. Therefore in the first simulation, we would expect the shell to stall if it was driven predominantly by the momentum, rather than energy, input from the quasar. In the other two simulations, the shell should escape to infinity. We present the results below, drawing particular attention to the dynamics of the self-gravitating clumps formed in the three simulations.

3 RESULTS

Figure 1 shows the column density for the simulation M5 and velocity vectors projected on to the plane of the figure for gas at 11.8 Myr after the quasar switches on. We see that while the bulk motion of the gas is radially outwards, there is a lot of structure forming as the shell fragments. This is essentially the same result as found by NZ12: the cooling time in the shocked ambient medium is $t_{\text{cool}} \simeq 4 \times 10^5 v_8 R_{\text{kpc}}^2 \text{ yr}$, where $v_8 = v_e/1000 \text{ km/s}$; this is a few times shorter than the flow timescale $R v_e \sim 10^6 \text{ yr}$, so the outer shell cools rapidly and is strongly compressed. In this simulation, the outflow does not stall, but rather keeps expanding and accelerating up to a radial velocity $v_r \simeq 2000 \text{ km/s}$. This is

because the SMBH mass is above the critical M_{σ} limit (eq. 1) and so even gas close to the SMBH is driven outside the cooling radius, where it can be accelerated further by the energy input. The network of filaments produces density enhancements that become self-gravitating.

In Figure 2, we show a narrow wedge projection (see NZ12 for more detail) of the simulation M2 at 7.09, 8.27 and 9.45 Myr. White squares show star particles. Note that they form filaments pointing mainly in the radial direction, similar to the “fingers of creation” found in NZ12. Denser gas regions experience a lower outward push per unit mass, and therefore lag slightly behind lower density gas. These dense filaments eventually collapse into self-gravitating clumps, which are then observed to lag behind the shell. Clumps born earlier on are born with lower radial velocity since the gas shell is being accelerated outward due to its decreasing mean projected column density. Therefore dense gas regions collapsing over the course of the simulations result in “streamers” of star particles clearly visible in Figure 2. For the simulation M2 in particular, the first clumps move with mean radial velocities $v_* \sim 200 \text{ km/s}$, slightly lower than the bulge escape velocity $v_{\text{esc}} \simeq 400 \text{ km/s}$ (see also red points in Figure 3).

Figure 3 shows the radial velocity versus radius for star particles formed in all three simulations. The snapshots are taken at 16.5 Myr for M1 and at 9.45 Myr for the other two simulations. The dashed line in the simulation shows the escape velocity as a function of radius, assuming the effective radius for the model galaxy of 20 kpc. In simulation M1, the shell fragments, the dense clumps stall and then fall back on to the SMBH. For this reason, there are both positive and negative radial velocities for stars in this simulation. Almost all of the stars formed in this simulation (blue dots) are bound to the host galaxy.

For the more massive SMBHs, the shell is continuously driven out. As the shell is of a finite mass, its mean projected column density decreases as it expands, and so quasar outflow can accelerate it to velocities larger than would be calculated analytically for a shell of infinite radius (see, e.g., King et al. 2011, for derivation). As already explained above, the collapsing star-forming clumps do not experience the same outward acceleration from the quasar outflow and decouple from the shell. Star particles born earlier are born with a lower outward velocity, therefore they lag behind those that are born at later time. As a result the dispersion in clump velocities increases with time, which is already evident from Figure 2. Figure 3 shows that some of the stars formed in simulation M2 are bound to the galaxy (those below the dashed curve); they move on very elongated, nearly radial orbits. Stars formed later have large enough radial velocities to escape the potential completely. In simulation M5 the whole of the shell is accelerated to velocities above the escape velocity before the stars are born; all of the newly made stars are on escaping trajectories.

A large fraction, 30 – 70%, of the initial mass of the shell is converted into star particles in each of the three simulations. As discussed in section 2, such a large star formation efficiency is clearly an overestimate. Star formation feedback, neglected here, is likely to reduce the total mass of the newly made stars. Nevertheless, even if star formation efficiency drops by an order of magnitude, e.g., to 5%, the total mass of stars formed on the radial outward tra-

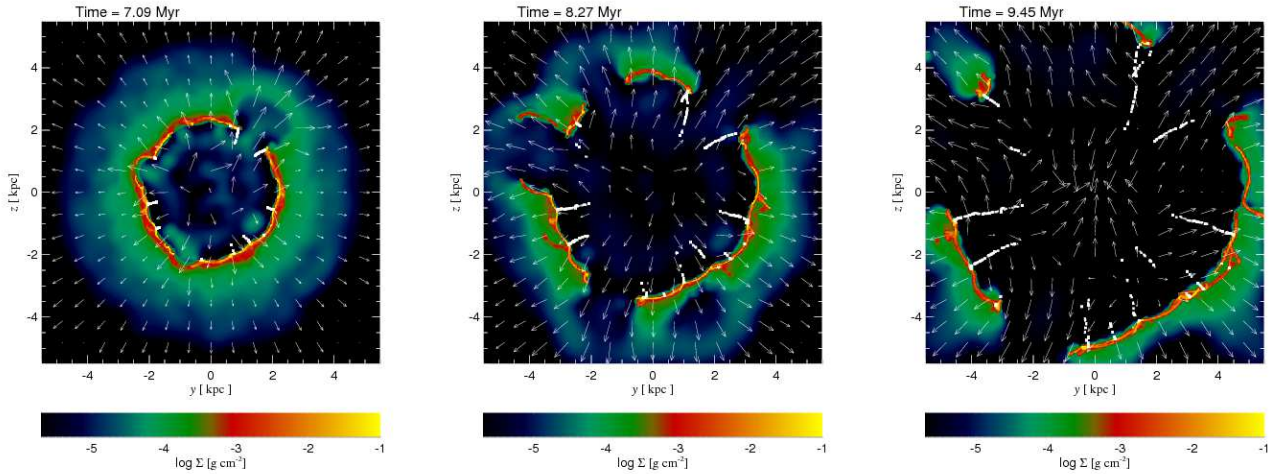


Figure 2. A wedge-slice through simulation M2 at times 7.09, 8.27 and 9.45 Myr (left to right panels, respectively). Colours show projected gas surface density, white squares represent star particles. Stars form from overdensities in the fragmenting shell, but their clusters are stretched out because the stars decelerate while the shell moves outwards with approximately constant velocity. Arrows are gas velocity vectors, giving qualitative information about the turbulence in gas motion induced by quasar feedback.

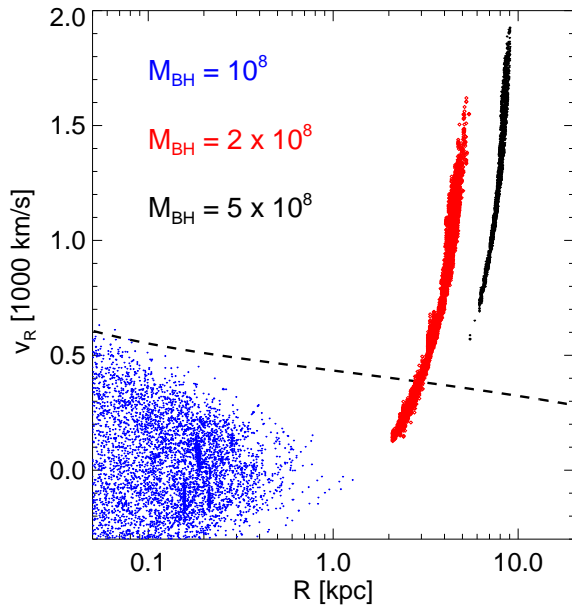


Figure 3. Radial velocity of stars formed in simulations M1, M2 and M5 versus their instantaneous radial coordinate, R . The dashed line shows the escape velocity as a function of R . The star forming shell created by the lightest black hole stalls at a radius of $R \sim 0.3$ kpc, so all of the stars formed in this simulation are bound to the host.

jectories would be between a few times $10^7 M_{\odot}$ to $10^8 M_{\odot}$. We also note that star formation efficiency is expected to be higher in compressed systems (Keto et al. 2005). Thus, provisionally, we may expect at least $\sim 10^8 M_{\odot}$ of stars to be formed.

4 DISCUSSION

The simulations presented here show that, in the setup explored, quasar feedback can expel gas from the bulge of its host galaxy with high velocity and simultaneously compress it to high densities. These two processes result in formation of hyper-velocity stars (HVS). The total mass of these stars is unclear at the moment, since our simulations neglect star formation feedback (see §2 and 3). In addition, here we explored the simplest possible initial conditions – a spherically symmetric gas distribution, with the density profile $\rho \propto 1/R^2$. Simulations of AGN feedback with more realistic non-spherical initial conditions show that the quasar outflow driven bubble may burst in directions of the lowest column depth of the ambient gas, e.g., perpendicular to the plane of the host galaxy (Nayakshin & Zubovas 2012). Feedback in such a geometry may be (Zubovas & Nayakshin 2012) the reason behind formation of the “Fermi Bubbles” in the Milky Way (Su et al. 2010). In such geometries the fraction of ambient gas put on hyper-velocity orbits is smaller, and therefore we expect that the total mass of the HVS would be also smaller.

Therefore, while we are confident that AGN feedback can launch HVS, we are currently unable to quantify how often this occurs in more realistic situations, and how large the fraction of gas turned into stars is. With this caveat in mind, we now discuss possible observational implications of HVS made by AGN feedback.

4.1 Radial mixing of stars and clouds

Stars formed in the shock driven outward by the quasar with velocities below the escape velocity, such as those shown with the red symbols that are below the dashed curve in Figure 3, are destined to fall back to the bulge. These stars are on very elongated nearly radial trajectories, and spend most of the time at large radii, i.e., $R \gtrsim$ a few to a few tens of kpc. These stars are thus unusual in that they were born from the gas initially filling the inner region of the

galaxy, the bulge, but due to their large radial velocity kicks now belong to the galactic halo. Such halo stars could thus stand out due to their highly radial orbits and (likely) higher metallicity compared to a typical low metallicity halo star. The most extreme of these stars, in the outskirts of the dark matter halos of their host galaxies, may provide a significant contribution to the intergalactic infrared background. It was recently shown that a 0.1% fraction of total galaxy light deposited into the outskirts of halos could explain most of the background radiation (Cooray et al. 2012); while we cannot quantify the total luminosity of stars expelled to such distances in our model, our results are consistent with this requirement.

The gas clumps expelled from the bulge do not necessarily all form stars. Some of these clumps may remain marginally bound, and collapse on a timescale longer than the cloud ejection timescale. In that case, the gas clumps can mix with the halo gas, joining the high velocity cloud (HVC) population. These clouds are observed all around the Milky Way, have high peculiar velocities and metallicities similar to or slightly lower than Solar (Wakker & van Woerden 1997; Wakker 2001). Their evolutionary timescales are estimated at a few tens to several hundred Myr, suggesting continuous replenishment, such as condensation from tidal streams (Putman et al. 2003b) or a galactic fountain (Bregman 1980; Kwak et al. 2009). Our simulations suggest that quasar outflow, long extinguished by now, could also contribute to production of HVCs.

4.2 Bulge disruption

It is usually assumed that gas is a small fraction of the total mass of the host, with the rest consisting of dark matter and stars. This is clearly correct for present day galaxies, and must be globally true for galaxies at birth since the universal baryon fraction is only $f_g \sim 0.16$. However, gas can collapse to the centre of the potential if its angular momentum is sufficiently low and so dominate the potential in the central region of the host. In this case, if most of the gas is driven rapidly out of the host, the remaining mass may be insufficient to bind the bulge gravitationally. It then has to expand and perhaps blend with the rest of the galaxy, adding stars to the halo, with faster stars leaving the host galaxy altogether.

In the extreme cases this should result in an SMBH without a clear parent bulge or an SMBH that appears to be far more massive than it should be based on the $M_{\text{bh}} - M_{\text{bulge}}$ relation. This cannot be a common outcome: based on Figure 3, we see that the SMBH mass needs to be somewhat above the M_σ value to drive the cold shell out before the latter collapses into stars. This happens even in a spherically-symmetric geometry, which is more conducive to large outflows; NZ12 found that for more realistic non-spherical geometries, AGN feedback in the gas rich epoch tends to compress and trigger star bursts in cold gas without driving the shell away.

Nevertheless, bulge destruction or erosion (partial destruction) by the SMBH feedback expelling a large fraction of the bulge mass may occasionally happen, especially for active galaxies in the early Universe and/or violently merging systems. This may be relevant for the recently observed population of SMBHs in bulgeless galaxies (Simmons et al. 2012; McAlpine et al. 2011; Araya Salvo et al. 2012) and

well as several SMBHs with masses significantly above those predicted by the black hole - bulge mass correlation (Bogdán et al. 2012).

4.3 Type II supernovae on galactic outskirts

The distance travelled by a star moving with radial velocity $v = 1000v_8 \text{ km s}^{-1}$ for time $t = 10^7 t_7 \text{ yrs}$ is

$$\Delta R = vt \approx 10 \text{ kpc } v_8 t_7 . \quad (2)$$

Stars with Solar or super-Solar metallicity that are more massive than $M \sim 8 M_\odot$ end their main sequence life in a Type II supernova explosion (Heger et al. 2003). The main sequence lifetime of stars of mass $M = 8 M_\odot$ is approximately 100 Myr, while the most massive stars, $M \gtrsim 50 M_\odot$ live only $\sim 4 \text{ Myr}$. Therefore we can expect that massive stars launched by the quasar outflow produce Type II supernovae at a distance from a few to few tens of kpc away from the galaxy's center. Additionally, long duration GRBs are expected from this flung-out population of stars (Woosley & Bloom 2006), potentially explaining the GRBs that are known to be offset, some by as much as $> 10 \text{ kpc}$, from the centres of their host galaxies (Bloom et al. 2002).

4.4 Reionisation and metal enrichment of the Universe

Bouwens et al. (2011) show that stars formed in galaxies at around the reionization epoch can provide sufficient amount of ionizing photons provided that they escape into intergalactic space efficiently enough. In particular, these authors estimate that an escape fraction of 20% is required for consistency with the WMAP results at the 2σ level. This is much higher than the escape fraction of only $\sim 1 - 2\%$ as found for the Milky Way (Putman et al. 2003a). The disagreement is all the more striking because the present day Milky Way contains very little gas per unit total mass of the Galaxy compared with the early star forming galaxies, which were also probably much more compact given that observations show that galaxies grew inside out at least from $z \sim 2$ to the present day (van Dokkum et al. 2010).

It is therefore interesting to note that the massive stars launched at high velocities, $v \gtrsim v_{\text{esc}}$, find themselves outside the cold high density gas environment of the inner galaxy. Ionizing photons emitted by these stars have orders of magnitude smaller average gas column depth to navigate through to escape from the galaxy's halo. Note that while massive stars are trailing the cold shell that created them earlier on, the shell is a web of thin dense filaments with most of the sky covered by a much lower density material (see Fig. 1 and also Fig. 2 in NZ12). Therefore, the escape fraction of ionising radiation for these stars may be much closer to unity than for the stars residing in the inner galaxy. The Hyper Velocity Stars (HVS) formed during quasar outflow ejection may thus be far more efficient in terms of reionization than the "normal" galactic stars, although it remains to be seen if a sufficient mass of HVS can be created to contribute significantly to the reionization of the Universe.

Lower mass stars ejected of their host galaxies at high velocities may be contributing to metal enrichment of the gas outside of galaxies. Their longer main sequence lifetime,

$t \sim 10^9$ yrs, implies that they may travel as far as ~ 1 Mpc (see eq. 2) from their hosts before ejecting their envelopes. Recent observations have discovered low-mass stars at distances of up to 2 Mpc from the centre of the Milky Way (Palladino et al. 2012). These stars might have been ejected by three-body interactions between a binary star and the central SMBH of the Milky Way (e.g., Yu & Tremaine 2003), but without knowledge of their orbits, it is impossible to confirm or disprove this scenario. The existence of these stars is also consistent with our model; they might have been ejected by a quasar outflow from the Milky Way several Gyr ago. Importantly, this “stellar outflow” may actually reach further into the intergalactic space than quasar gas outflows. Here we found that stars are lagging behind gas outflows while quasar outflow provides an outward acceleration for the gas shell; but eventually the quasar must turn off, and the gas outflow must decelerate faster than a HVS because the outflow interacts with intergalactic medium by a shock whereas the stars continue to travel ballistically.

5 SUMMARY AND CONCLUSION

Using numerical simulations of SMBH feedback upon gas in its host galaxy, we have shown that quasars may not only trigger star formation in their host bulges (as shown by Nayakshin & Zubovas 2012), but also expel a fraction of these newly-formed stars from the host galaxy. Expulsion requires a large SMBH mass ($M > M_\sigma$), so may not be a common phenomenon. Further modelling is needed to determine the mass fraction produced in this HVS population, since its potential implications are wide ranging.

Stars originating in the bulge launched at high velocities on nearly radial trajectories may completely escape the galaxy; slower stars add a metal-rich subpopulation in the region and may contribute to the intergalactic light. High metallicity HVS produce ionising radiation and so may contribute to the reionisation of the Universe; they also explode as supernovae, potentially contributing to Type II supernovae on galactic outskirts. Lower mass stars travel further out, enriching the extragalactic medium with metals. Finally, a significant fraction of the galaxy bulge mass may become unbound due to such “stellar outflows”, leading to SMBHs in bulgeless galaxies or SMBHs with masses much higher than expected from the black hole - bulge mass relation. We conclude that quasar outflows shape the properties of their galaxies and surrounding medium in many ways, not just by removing gas and quenching star formation, as usually acknowledged.

ACKNOWLEDGMENTS

This research used the ALICE High Performance Computing Facility at the University of Leicester. Some resources on ALICE form part of the DiRAC Facility jointly funded by STFC and the Large Facilities Capital Fund of BIS. Theoretical astrophysics research in Leicester is supported by an STFC Rolling Grant.

REFERENCES

- Araya Salvo C., Mathur S., Ghosh H., Fiore F., Ferrarese L., 2012, *ApJ*, 757, 179
 Bloom J. S., Kulkarni S. R., Djorgovski S. G., 2002, *AJ*, 123, 1111
 Bogdán Á., Forman W. R., Zhuravleva I., et al., 2012, *ApJ*, 753, 140
 Booth C. M., Schaye J., 2009, *MNRAS*, 398, 53
 Bouwens R. J., Illingworth G. D., Oesch P. A., et al., 2011, *ApJ*, 737, 90
 Bregman J. N., 1980, *ApJ*, 236, 577
 Cooray A., Smidt J., de Bernardis F., et al., 2012, *Nature*, 490, 514
 Di Matteo T., Springel V., Hernquist L., 2005, *Nature*, 433, 604
 Dubois Y., Devriendt J., Slyz A., Teyssier R., 2012, *MNRAS*, 420, 2662
 Feruglio C., Maiolino R., Piconcelli E., et al., 2010, *A&A*, 518, L155
 Gaibler V., Khochfar S., Krause M., Silk J., 2012, *MNRAS*, 425, 438
 Heger A., Fryer C. L., Woosley S. E., Langer N., Hartmann D. H., 2003, *ApJ*, 591, 288
 Kennicutt Jr. R. C., 1998, *ApJ*, 498, 541
 Keto E., Ho L. C., Lo K.-Y., 2005, *ApJ*, 635, 1062
 King A., 2003, *ApJL*, 596, L27
 King A., 2005, *ApJL*, 635, L121
 King A. R., Zubovas K., Power C., 2011, *MNRAS*, 415, L6
 Kwak K., Shelton R. L., Raley E. A., 2009, *ApJ*, 699, 1775
 Larson R. B., 1969, *MNRAS*, 145, 271
 McAlpine W., Satyapal S., Gliozzi M., Cheung C. C., Samburina R. M., Eracleous M., 2011, *ApJ*, 728, 25
 Nayakshin S., Cha S.-H., Hobbs A., 2009, *MNRAS*, 397, 1314
 Nayakshin S., Cuadra J., Springel V., 2007, *MNRAS*, 379, 21
 Nayakshin S., Power C., 2010, *MNRAS*, 402, 789
 Nayakshin S., Power C., King A. R., 2012, *ApJ*, 753, 15
 Nayakshin S., Zubovas K., 2012, *ArXiv e-prints*
 Palladino L. E., Holley-Bockelmann K., Morrison H., et al., 2012, *AJ*, 143, 128
 Pounds K. A., King A. R., Page K. L., O’Brien P. T., 2003a, *MNRAS*, 346, 1025
 Pounds K. A., Reeves J. N., King A. R., Page K. L., O’Brien P. T., Turner M. J. L., 2003b, *MNRAS*, 345, 705
 Pounds K. A., Vaughan S., 2011, *MNRAS*, 413, 1251
 Proga D., 2003, *ApJ*, 585, 406
 Putman M. E., Bland-Hawthorn J., Veilleux S., Gibson B. K., Freeman K. C., Maloney P. R., 2003a, *ApJ*, 597, 948
 Putman M. E., Staveley-Smith L., Freeman K. C., Gibson B. K., Barnes D. G., 2003b, *ApJ*, 586, 170
 Rupke D. S. N., Veilleux S., 2011, *ApJL*, 729, L27
 Shakura N. I., Sunyaev R. A., 1973, *A&A*, 24, 337
 Silk J., Antonuccio-Delogu V., Dubois Y., et al., 2012, *A&A*, 545, L11
 Silk J., Rees M. J., 1998, *A&A*, 331, L1
 Simmons B. D., Lintott C., Schawinski K., et al., 2012, *ArXiv e-prints*
 Springel V., Di Matteo T., Hernquist L., 2005, *MNRAS*, 361, 776

- Sturm E., González-Alfonso E., Veilleux S., et al., 2011, *ApJL*, 733, L16
- Su M., Slatyer T. R., Finkbeiner D. P., 2010, *ApJ*, 724, 1044
- Tombesi F., Cappi M., Reeves J. N., et al., 2010a, *A&A*, 521, A57+
- Tombesi F., Sambruna R. M., Reeves J. N., et al., 2010b, *ApJ*, 719, 700
- van Dokkum P. G., Whitaker K. E., Brammer G., et al., 2010, *ApJ*, 709, 1018
- Wakker B. P., 2001, *ApJS*, 136, 463
- Wakker B. P., van Woerden H., 1997, *ARA&A*, 35, 217
- Woosley S. E., Bloom J. S., 2006, *ARA&A*, 44, 507
- Yu Q., Tremaine S., 2003, *ApJ*, 599, 1129
- Zubovas K., King A., 2012a, *ApJL*, 745, L34
- Zubovas K., King A. R., 2012b, *MNRAS*, 426, 2751
- Zubovas K., Nayakshin S., 2012, *MNRAS*, 424, 666